

Gravitational stability of simply rotating Myers-Perry black holes: tensorial perturbations

Hideo Kodama*

Cosmophysics Group, IPNS, KEK and the Graduate University of Advanced Studies, 1-1 Oho, Tsukuba 305-0801, Japan

R. A. Konoplya†

*Department of Physics, Kyoto University, Kyoto 606-8501, Japan
Theoretical Astrophysics, Eberhard-Karls University of Tübingen, Tübingen 72076, Germany*

Alexander Zhidenko‡

*Instituto de Física, Universidade de São Paulo
C.P. 66318, 05315-970, São Paulo-SP, Brazil*

We study the stability of $D \geq 7$ asymptotically flat black holes rotating in a single two-plane against tensor-type gravitational perturbations. The extensive search of quasinormal modes for these black holes did not indicate any presence of growing modes, implying the stability of simply rotating Myers-Perry black holes against tensor-type perturbations.

PACS numbers: 04.30.Nk, 04.50.+h

I. INTRODUCTION

Higher-dimensional gravity appears in the landscape of modern physics as a result of the string theory or in various brane-world models. Both, string theory and brane-world contexts imply the existence of higher dimensional black holes. For the four dimensional gravity, there exists a uniqueness theorem that states that the asymptotically flat stationary black hole is described by the well-known Kerr solution. In higher dimensions, such a uniqueness theorem does not hold any more, but a great variety of solutions describing black objects, such as black holes, strings, branes, rings, saturns, exist instead [1]. Therefore, the stability of rotating black holes in higher than four space-time dimensions is an open appealing problem [3], [4]. Stability could help to select among the variety of "black" solutions those which could be realized in nature. Another motivation to study the evolution of higher-dimensional black hole perturbations comes from the possibility to observe mini-black holes in future experiments with cosmic showers or in the Large Hadron Collider [2].

The stability of spherically symmetric static black holes has been intensively studied in recent few years. It started from the papers by Ishibashi and Kodama [6], [7], [8], who, using the gauge-invariant formalism [5], proved that the D -dimensional generalization of the Schwarzschild black hole, described by the Tangherlini metric, is stable. Then, the stability of higher-dimensional black holes allowing for a cosmological constant was shown in [9] for $D = 5, 6, \dots, 11$ Schwarzschild-

de Sitter (SdS) and in [10] for $D = 5, 6, \dots, 11$ Reissner-Nordström-anti-de Sitter (RNAdS) black holes. The D -dimensional Reissner-Nordström black hole was shown to be stable, although Reissner-Nordström-de Sitter black holes proved to be unstable in higher than six space-time dimensions [11], when both the charge and Λ - term are large enough. The stability of black holes in higher dimensional generalizations of the Einstein gravity, such as the Gauss-Bonnet and Lovelock theories, was considered in [12], [13], [14], and an instability for large values of the Gauss-Bonnet coupling α was found. This Gauss-Bonnet instability was shown to have quite peculiar behavior: the instability starts dominating after a long period of damped quasinormal oscillations. In addition, the stability analysis and time domain evolution of perturbations were considered for the Kaluza-Klein type solutions, such as (squashed) Kaluza-Klein black holes [15] or black strings [16].

While the stability of static black holes in higher dimensions is relatively well studied, the stability of rotating black holes for $D > 4$ is still an open question, because the separation of variables for all types of perturbations is a complicated problem. Nevertheless, some particular results have been obtained for the Myers-Perry black holes with all equal angular momenta, though only for either tensor-type perturbations [18] or for the so-called zero mode [19].

In our previous paper [21], we have started the investigation of gravitational perturbations of a much more interesting type of higher-dimensional rotating black holes, simply rotating black holes. These black holes have only one non-vanishing angular momentum component and are rotating in a single two-plane. Thus, they can be interpreted in brane-world scenarios as black holes created in particle collisions occurred on our brane. The perturbation equations for the $D > 6$ dimensional simply rotating black holes, allowing for a cosmological con-

*Electronic address: Hideo.Kodama@kek.jp

†Electronic address: konoplya.roma@yahoo.com

‡Electronic address: zhidenko@fma.if.usp.br

stant, were reduced in [21] to the wave-like form, and gravitational spectrum of asymptotically-AdS solutions was considered. The asymptotically AdS rotating black holes proved to be gravitationally unstable on superradiant modes only, and with a tiny instability growth rate [21].

In the present paper we shall continue research that started in [21] and consider tensor-type gravitational spectrum of asymptotically flat, Myers-Perry black holes. The quasinormal modes beside their importance for stability proof, may have useful implications for the study of the evolution of mini higher-dimensional black holes,

because quasinormal modes dominate at late time of the bolding phase [2] of an evaporating black hole.

Using the Frobenius method for the angular part of the perturbation equations and both WKB and Frobenius methods for the radial part, we have found the quasinormal modes of simply-rotating Myers-Perry black holes. The paper is organized as follows: Sec. II gives basic information on simply-rotating MP black holes. Sec. III is devoted to description of the numerical methods that we used for finding the quasinormal modes. Sec. IV discusses the obtained numerical results.

II. BASIC FORMULAS

The metric for the higher-dimensional Myers-Perry black hole can be written in the Boyer-Lindquist coordinates as

$$ds^2 = \frac{1}{\rho^2} \left[\frac{2M}{r^{n-1}} - \rho^2 \right] dt^2 - \frac{4aM \sin^2 \theta}{\rho^2 r^{n-1}} dt d\phi + \frac{\sin^2 \theta}{\rho^2} \left[(r^2 + a^2) \rho^2 + \frac{2a^2 M}{r^{n-1}} \sin^2 \theta \right] d\phi^2 + \frac{\rho^2}{\Delta} dr^2 + \rho^2 d\theta^2 + r^2 \cos^2 \theta d\Omega_n^2, \quad (1)$$

where $n = D - 4$, $d\Omega_n^2$ is the metric of the n -dimensional unit sphere, and

$$\Delta := (r^2 + a^2) - \frac{2M}{r^{n-1}}, \quad \rho^2 := r^2 + a^2 \cos^2 \theta. \quad (2)$$

Here M is the mass of the black hole and a is the angular momentum per unit mass.

The equations for the tensor-type gravitational perturbations of this black hole are reduced to the coupled equations [21] for the angular part

$$2(1 - x^2)S''(x) + (-1 + n - (3 + n)x)S'(x) + \left(\frac{\mu}{2} + \frac{a^2 \omega^2 (x - 1)}{4} + \frac{m^2}{x - 1} - \frac{\ell(\ell + n - 1)}{1 + x} \right) S(x) = 0, \quad (3)$$

$$x = \cos(2\theta), \quad n = 3, 4, 5, \dots, \quad \ell = 2, 3, 4, \dots, \quad m = 0, \pm 1, \pm 2, \dots,$$

and for the radial part

$$\frac{d^2 P(r)}{dr_\star^2} + Q(r)P(r) = 0, \quad (4)$$

$$Q(r) = \left(\omega - \frac{2Mam}{(r^2 + a^2)^2 r^{n-1}} \right)^2 - \frac{\Delta(r)}{(r^2 + a^2)^2} \left(\mu - \frac{a^2 m^2}{(r^2 + a^2)^2} \left\{ r^2 + a^2 + \frac{2M}{r^{n-1}} \right\} + \frac{n(n+2)}{4} + \left(l + \frac{n}{2} \right) \left(l + \frac{n}{2} - 1 \right) \frac{a^2}{r^2} + \frac{a^2}{r^2 + a^2} + \frac{\{(n+2)r^2 + na^2\}^2 - 8a^2 r^2}{2(r^2 + a^2)^2} \frac{M}{r^{n+1}} \right). \quad (5)$$

with respect to the frequency ω and the separation constant μ . Here, we have defined the tortoise coordinate r_\star as

$$dr_\star = \frac{r^2 + a^2}{\Delta(r)} dr.$$

III. NUMERICAL METHOD FOR FINDING OF THE QUASINORMAL SPECTRUM

A. The angular part

The differential equation for the angular part (3) can be solved numerically in the same way as it was done

in [22]. Namely, the second-order differential equation (3) is reduced to an algebraic equation with an infinite

continued fraction [21]. This equation can be solved numerically to determine the separation constant μ for each value of ω . Thus, we can find numerically the function $\mu_j(\omega)$, where $j = 0, 1, 2, \dots$ is an integer number.

The number j enumerates the eigenvalues of μ . If the black hole does not rotate ($a = 0$), the equation for the angular part can be solved exactly to yield [21]

$$\mu = (2j + \ell + |m|)(\ell + 2j + |m| + n + 1), \quad (6)$$

which coincides with the eigenvalue for the harmonic function on the unit $(n + 2)$ -sphere, with the multi-pole number $(2j + \ell + |m|) = 2, 3, 4, \dots$

If the rotation parameter a is non-vanishing, the eigenvalues μ are non-integer and complex. For any value of ω , we can enumerate them by the non-negative integer j in the following way.

1. We start from the non-rotating black hole and find exactly the value of μ for the corresponding j .
2. We increase the rotation parameter by a very small value and search for the closest to the previously found solution for μ .
3. We repeat the previous step until any required value of a is reached.

In this way we are able to enumerate the values of the separation constant μ for any ω and a . In order to decrease the computation time, in practice, when searching for quasi-normal modes, we start from the known values

of the quasi-normal frequencies for a non-rotating black hole [27] and, increasing step by step the value of a , find the closest pair of μ and ω to the previously found one. An alternative approach for the computation of the angular separation constant has been recently suggested in [28].

B. The radial part

In order to simplify our notations, we will parameterise the black hole mass by the black hole horizon radius r_+ :

$$2M = r_+^{n-1}(r_+^2 + a^2). \quad (7)$$

In solving the radial part of the perturbation equation, we use two alternative approaches: the numerical Frobenius method [23] and the semi-analytical JWKB approximation [25].

Let us start from the description of the Frobenius method. We are searching for the solution of the equation (4) with the quasi-normal boundary conditions that requires pure in-coming waves at the event horizon and pure out-going waves at spatial infinity. For a black hole in the asymptotically flat background, they imply a purely ingoing wave at the event horizon r_+ and purely outgoing wave at the spatial infinity. If $P(r)$ satisfies the quasi-normal boundary conditions, then it can be written in the following form

$$P(r) = \left(1 - \frac{r_+}{r}\right)^{-i} \left(\omega - \frac{2Mam}{(r_+^2 + a^2)^2 r_+^{n-1}}\right) \frac{r_+^2 + a^2}{\Delta'(r_+)} \times \frac{\sqrt{r^2 + a^2}}{r} \times e^{i\omega r} \times F(r), \quad (8)$$

where $F(r)$ is a regular function at the event horizon $r = r_+$ and at the spatial infinity $r = \infty$.

In order to expand $F(r)$ in the convergent series in the region outside the event horizon, we choose the variable

$$z = \frac{r - r_+}{r - r_i},$$

where $r_i < r_+$ is chosen so that all the singular points of the equation (4), except the event horizon and the spatial infinity, are located outside the unit circle $|z| > 1$. These singular points satisfy the equation

$$\Delta(r) = 0.$$

Fortunately, the structure of the singular points allows us to fix r_i for a physically reasonable range of parameters.

After the value of r_i is fixed, we expand the function

F into the series

$$F(z) = \sum_{k=0}^{\infty} b_k z^k. \quad (9)$$

Substituting (9) and (8) into (4), we find the recurrence relation for the series coefficients b_i . Following [24], we are able to find the equation with an infinite continued fraction with respect to ω , which can be solved numerically.

The Frobenius method, being based on a convergent procedure, allows us to find quasinormal modes (QNMs) with any required accuracy, at least theoretically. Practically, for some range of parameters (in particularly for large azimuthal numbers) the convergence is too slow and the calculation cannot be easily done by a personal computer. In the range of parameters of slow Frobenius convergence, we use the WKB approximation [25]. The

WKB formula (10) was effectively used in a lot of papers [29], and here the WKB accuracy will be checked with the help of the Frobenius method. The 6-th order WKB formula reads

$$\frac{iQ_0}{\sqrt{2Q_0''}} - \sum_{i=2}^{i=6} \Lambda_i = N + \frac{1}{2}, \quad N = 0, 1, 2, \dots, \quad (10)$$

where the correction terms Λ_i were obtained in [25] and [26]. Here Q_0 and Q_0'' denote values of Q and its second derivative at its maximum with respect to the tortoise coordinate r_* , respectively. Since the function $\mu(\omega)$ is found only numerically, in order to find the roots of (10), we use the following algorithm:

1. For a given value of ω , we find the value of μ using the technique described in the section III A.
2. We substitute the numerical values of ω and μ into (5) and find Q as a complex analytical function of r .
3. The analytical continuation of the WKB formula into the complex plane implies that “maximum” of the potential peak is a complex value, which must be correctly chosen among the extrema of the potential Q . Since the WKB formula provides a sufficient accuracy only when $Re(\omega) \gtrsim Im(\omega)$, we will not consider the case, when the imaginary part of the quasi-normal frequency is large. Fortunately, when the imaginary part of ω is small, the imaginary part of μ is just a correction to its real part. Therefore, the real part of $Q(r)$ is much larger than its imaginary part, and the analytical continuation of the potential peak is trivial. We choose the location r_{ext} of the extremum of $Q(r)$, with a real part that is larger than the value of the event horizon and, at the same time, has the smallest imaginary part. This choice of the potential peak does not lead to any ambiguities for the considered parametric range, is close to the real potential peak for the non-rotating case and its searching can be easily programmed.
4. After the potential peak is fixed, we compare the frequency ω_{WKB} found with the formula (10) with our initial guess ω .

We search for the numerical minimum of the absolute value of the difference between the initial guess and the WKB formula $|\omega_{WKB}(\omega) - \omega|$, which is a function that can be calculated numerically using the above technique.

IV. QUASINORMAL MODES AND STABILITY

When we write the quasinormal frequency ω as

$$\omega = Re(\omega) + iIm(\omega), \quad (11)$$

$Im(\omega) > 0$ corresponds to an unstable (growing) mode, and $Im(\omega) < 0$ corresponds to a stable (damped) mode.

The quasinormal modes of a higher-dimensional simply rotating black hole are labeled by the quantum numbers ℓ , m and j , and also depend on the black hole parameters M and a as well as on the number of space-time dimensions D . Thus, the dependence of the spectrum on the above six parameters must be carefully considered in order to discard or observe instability. We have limited the calculations to $D = 7, 8, 9, 10$ and 11 . Keeping the event horizon radius r_+ fixed, we can measure the QN frequencies in units r_+^{-1} . Thus, the dependence of the quasinormal behavior on the four essential parameters must be studied. As all of them ℓ , m , j , a are not limited, in principle, we have to check the QN frequency as a function of each parameter starting from its minimal value and until reaching the *asymptotic region* where the frequency function does not change its behavior qualitatively. However, this task would require us to show here hundreds of plots and would take enormous computer time. Therefore, we were obliged to adopt the following practical strategy. If the frequency ω as a function of some parameter does not show any tendency to instability and the lowest (longest lived) modes stay very far from the instability region, we stopped the calculation at some reasonable value of the parameter. Strictly speaking, this does not allow us to establish mathematically rigorous proof of stability, but rather only give a numerical evidence of stability. In presenting the obtained results, in order to reduce the number of plots, we selected most representative ones with qualitatively different behavior. If plots are similar (for instance for various D and the same other parameters) we have shown only one representative plot of the whole “class”.

Comparison of the accurate data obtained by the Frobenius method with the WKB values shows that the WKB approximation becomes better as the azimuthal number m becomes larger, because it corresponds to larger values of the real part of the QN frequency. Indeed, the WKB approximation works when $|Re(\omega)| \gg |Im(\omega)|$. Thus, the limit of perfect WKB accuracy, which corresponds to the geometric optics approximation, should be achieved at $m \rightarrow \infty$.

Figures 1, 2 and 4 show the dependence of the quasinormal frequency, obtained by the Frobenius method, on the rotation parameter a for a few low values of m and the lowest values of ℓ and j . QNMs for a few low values of ℓ and j can be found in Figure 5. There, one can see that $Re(\omega)$ almost monotonically decreases (except for a small peak at very small a), when a is increased, while $Im(\omega)$ is growing until reaching its maximum, and then falling off to some asymptotic constant value. As the absolute value of $Im(\omega)$ decreases when m increases, it is important to find QNMs for sufficiently large m , in order to rule out the instability. On figures Fig. 6 one can see the high m behavior for a fixed a and D . Apparently $Re(\omega)$ is equidistant in the limit $m \rightarrow \infty$. The absolute value of $Im(\omega)$ approaches some maximum and

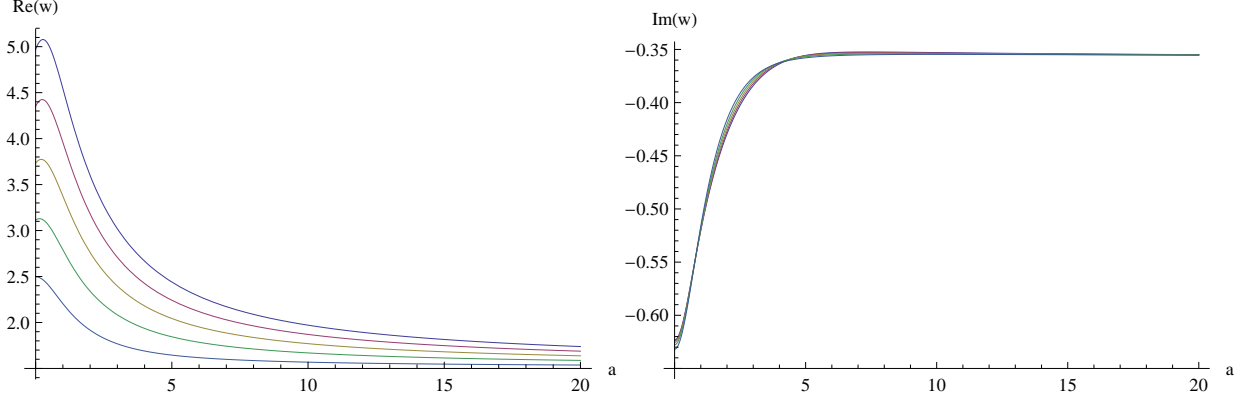


FIG. 1: Quasinormal modes as a function of a obtained by the Frobenius method for $D = 7$, $l = 2$, $j = 0$: $m = 4$ (blue), $m = 3$ (red), $m = 2$ (yellow), $m = 1$ (green), $m = 0$ (light blue). Higher values of m correspond to larger real part of ω .

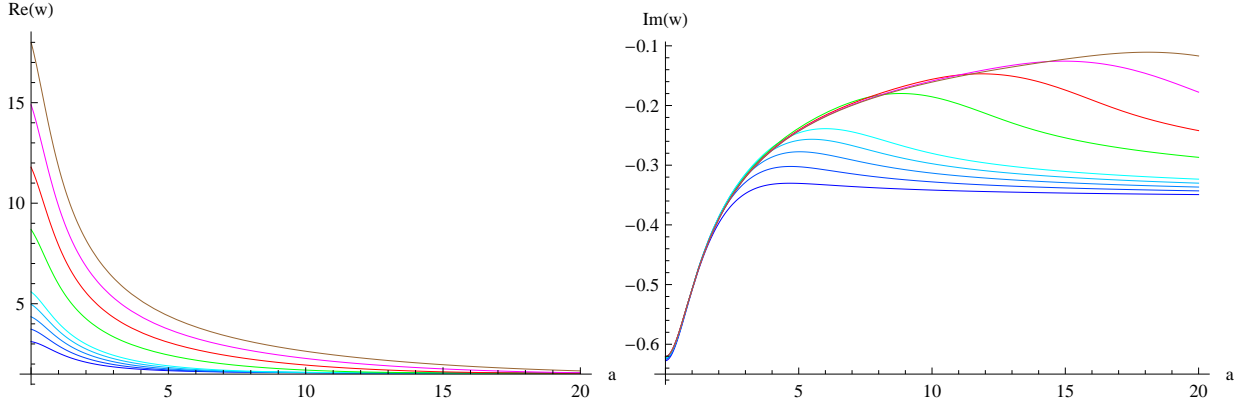


FIG. 2: Quasinormal modes obtained by the Frobenius method for $D = 7$, $l = 2$, $j = 0$: $m = -1$ (blue), $m = -2$, $m = -3$, $m = -4$, $m = -5$ (light blue), $m = -10$ (green), $m = -15$ (red), $m = -20$ (magenta), $m = -25$ (brown). Higher negative values of m correspond to the larger real and imaginary part of ω . The imaginary part of the QN frequency stays negative, implying stability against perturbations with the high negative azimuthal number m .

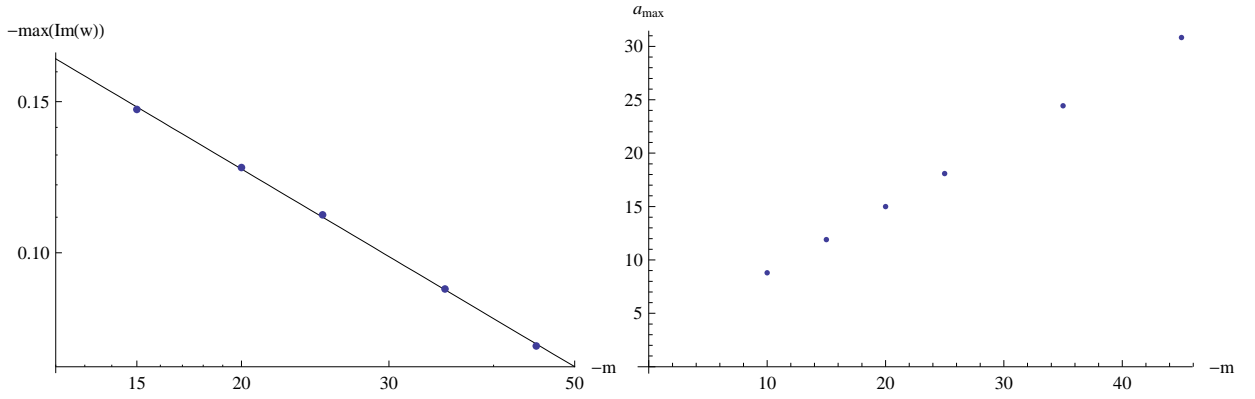


FIG. 3: Maximum value of the imaginary part of the quasi-normal mode for negative values of m together with the found fit $\max(\text{Im}(\omega)) \propto (-m)^{-\alpha}$ ($\alpha > 0$) for $D = 7$, $l = 2$, $j = 0$ (left figure, log-log scale) and corresponding values of the rotation parameter a_{\max} as a function of $-m$ (right figure).

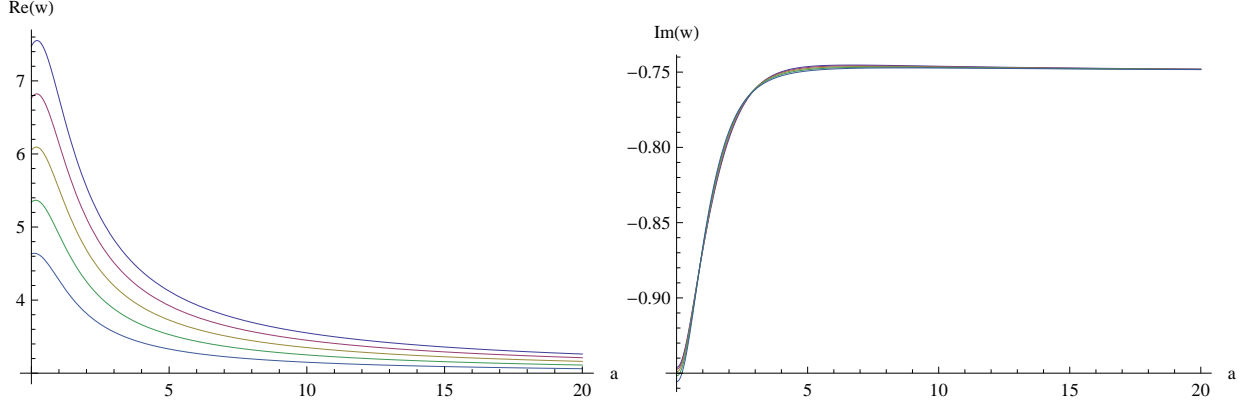


FIG. 4: Quasinormal modes obtained by the Frobenius method for $D = 10$, $l = 2$, $j = 0$: $m = 5$ (blue), $m = 4$ (red), $m = 3$ (yellow), $m = 2$ (green), $m = 1$ (light blue). Higher values of l correspond to larger real part of ω .

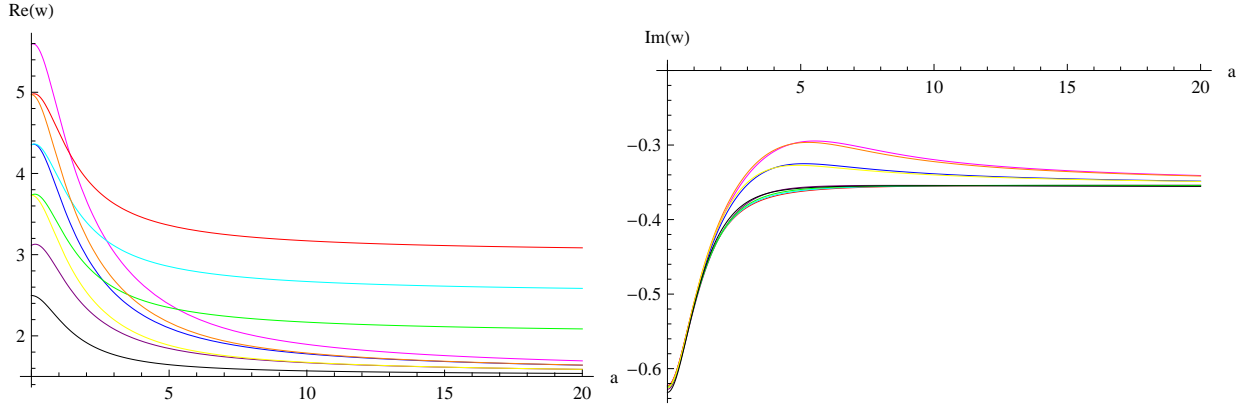


FIG. 5: Quasinormal modes obtained by the Frobenius method for $D = 7$: $(l = 2, m = 0, j = 0)$ - black, $(l = 2, m = 0, j = 1)$ - yellow, $(l = 2, m = 0, j = 2)$ - orange, $(l = 2, m = 1, j = 0)$ - purple, $(l = 2, m = 1, j = 1)$ - blue, $(l = 2, m = 1, j = 2)$ - magenta, $(l = 3, m = 1, j = 0)$ - green, $(l = 4, m = 1, j = 0)$ - cyan, $(l = 5, m = 1, j = 0)$ - red. The larger values of j correspond to the smaller values of the imaginary part of ω . The real part increases with $l + m + 2j$ for small rotation. When a is large, the real part for the multipole index $j \neq 0$ approaches zero, while that for $j = 0$ approaches a constant that increases with l .

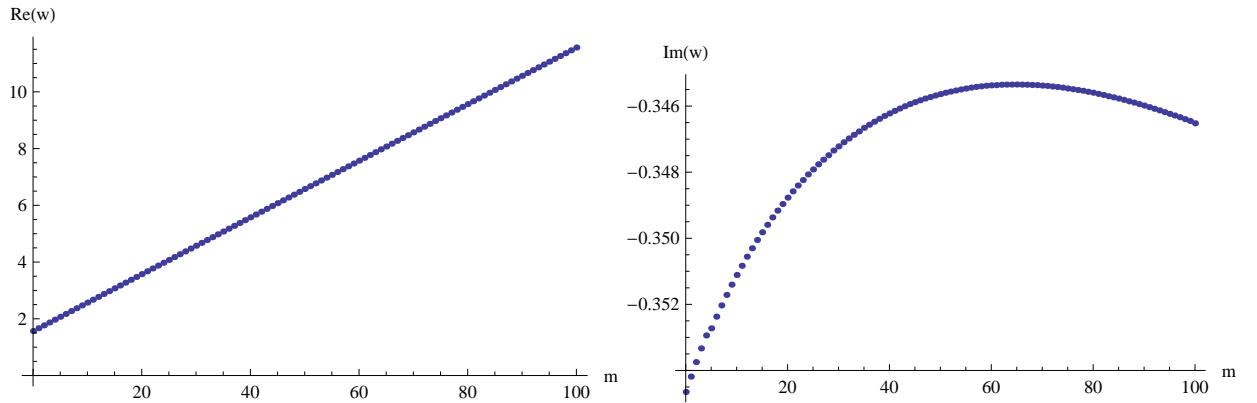


FIG. 6: Dependence of quasinormal modes obtained by the WKB method on the azimuthal number m for $D = 7$, $l = 2$, $j = 0$, $a = 10$.

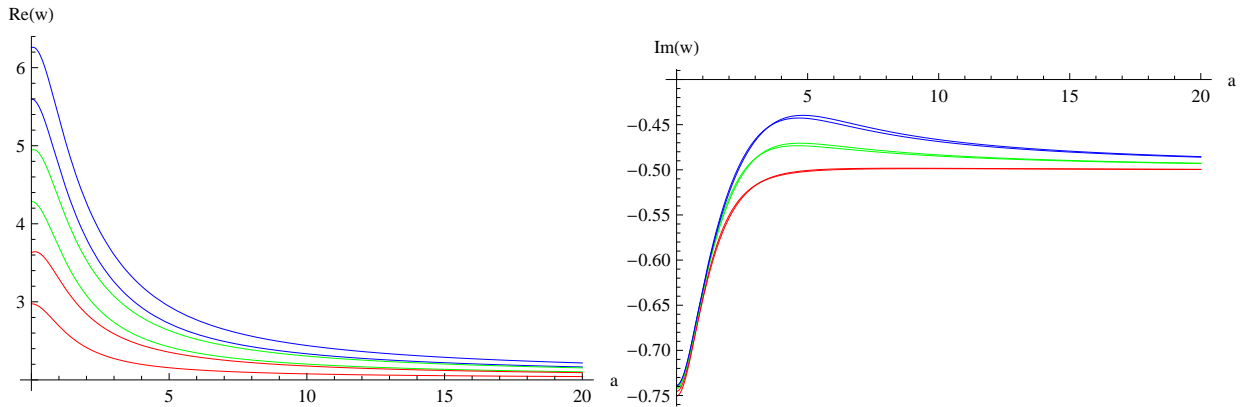


FIG. 7: Quasinormal modes as a function of a for $D = 8$, $l = 2$, $m = 0, 1$: $j = 0$ (red), $j = 1$ (green), $j = 2$ (blue). Higher m and j have larger real and imaginary part of ω

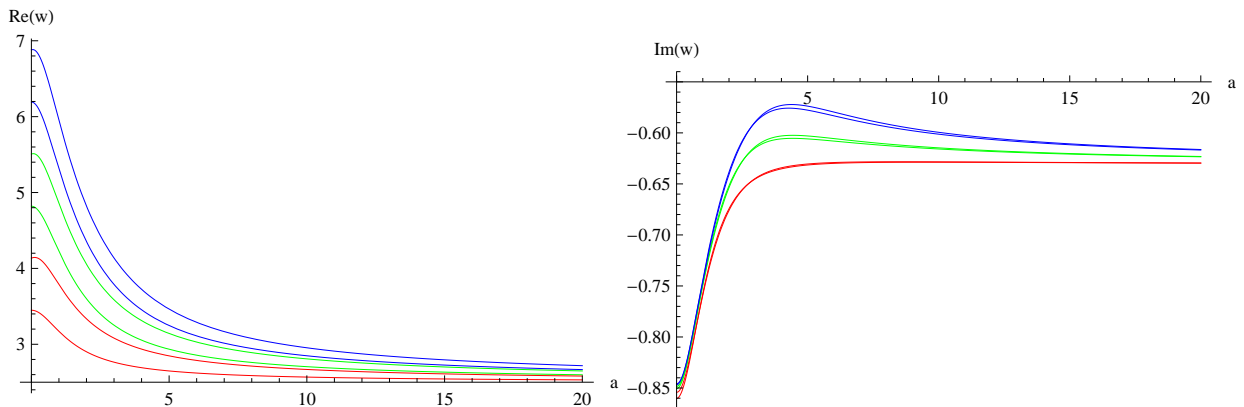


FIG. 8: Quasinormal modes as a function of a for $D = 9$, $l = 2$, $m = 0, 1$: $j = 0$ (red), $j = 1$ (green), $j = 2$ (blue). Higher m and j have larger real and imaginary part of ω .

then starts to fall off at large m , reaching some constant value asymptotically (see Fig. 6).

In the figure 2 one can see that for large negative m the maximum of the imaginary part is higher (closer to zero) and occurs for larger value of the rotation parameter a . One might ask himself if there is sufficiently high value of m for which the imaginary part crosses zero at some point leading to the instability for larger values of a . Our calculations show that this does not take place. In the left figure 3 we plot the dependence of the maximum value of $\text{Im}(\omega)$ as a function of $-m$ in the logarithmic-logarithmic scale. We see that this value is well approximated by the potential law $\max(\text{Im}(\omega)) \propto (-m)^{-\alpha}$ ($\alpha > 0$). If this is valid for the asymptotically large values of m , the maximum of the imaginary part of the quasi-normal frequency approaches zero only asymptotically. The corresponding value of the rotation parameter depends linearly on m and, therefore, also approaches infinity (see the right figure 3). Thus, we conclude that at least for the finite rotation parameter all modes of negative m are stable.

In figures 7, 8, 9, 10 the dependence of QNMs on j is shown. There, one can see that the QN spectrum stays well far from the instability point. Thus, we con-

clude that no growing mode was found for simply rotating Myers-Perry black holes with $D = 7, 8, 9, 10$ and 11, i.e. tensor-type gravitational perturbations are stable in the above cases.

V. CONCLUSIONS

We have investigated the stability of simply rotating Myers-Perry black holes with $D \geq 7$ against tensor-type gravitational perturbations. We have not found a growing mode, which apparently signifies stability against tensor perturbations.

In addition, we gave here extensive numerical data for the quasinormal frequencies for the tensor-type gravitational perturbations of these black holes.

Let us note that the quasinormal spectrum of a simply rotating Myers-Perry black hole is not a limit of that of a MP black hole in the AdS spacetime, when the AdS radius R approaches infinity. From the equation (71) of [21], one can see, that when $R \gg r_+$ the quasinormal

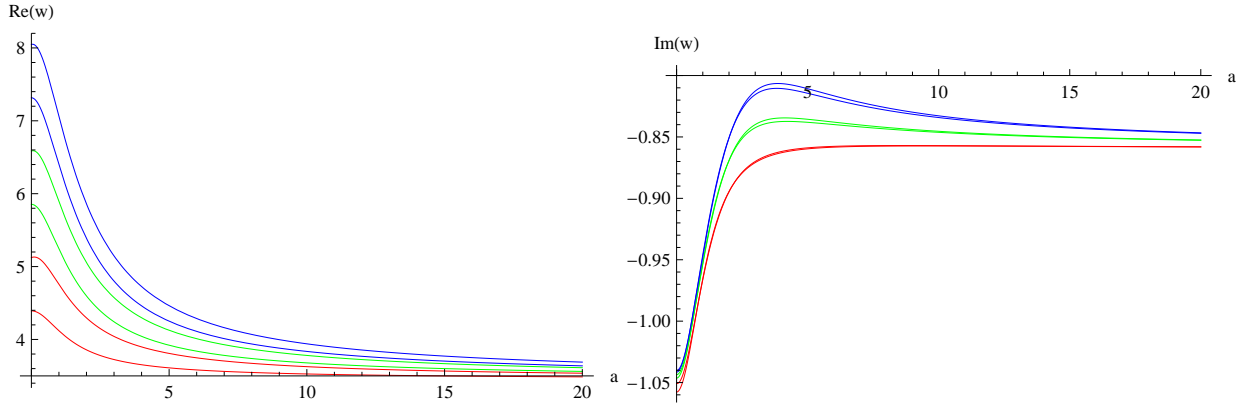


FIG. 9: Quasinormal modes as a function of a for $D = 11$, $l = 2$, $m = 0, 1$: $j = 0$ (red), $j = 1$ (green), $j = 2$ (blue). Higher m and j have larger real and imaginary part of ω .

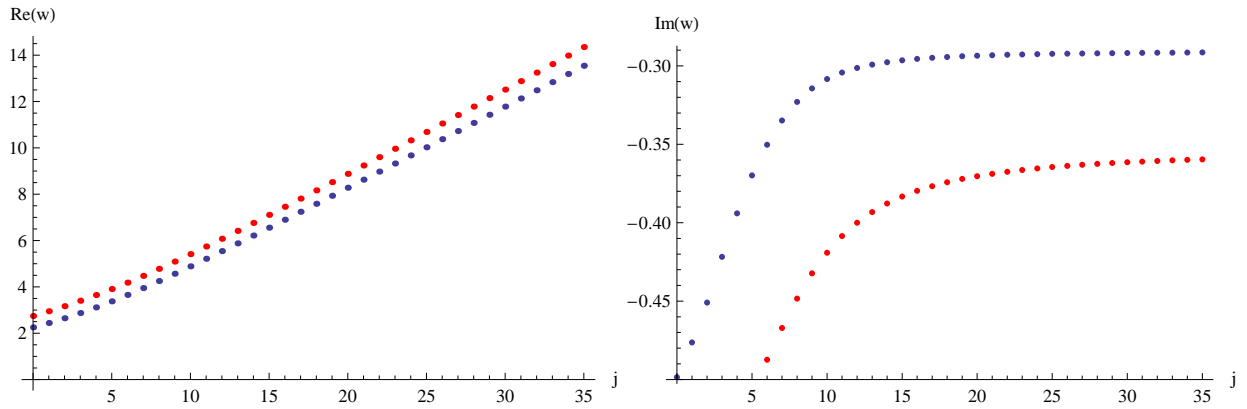


FIG. 10: Dependence of the quasinormal modes on j for $D = 8$ (blue) and $D = 9$ (red), $a = 7$, $m = 1$. The plots with larger $Re(\omega)$ and $Im(\omega)$ correspond to the larger D .

modes approach zero as

$$\begin{aligned} \omega &\sim \frac{2n + D + 2l + m + j - 1 + F(D, l, m, j, a)}{R} = \\ &= \mathcal{O}\left(\frac{1}{R}\right). \end{aligned}$$

In the forthcoming paper [30], we shall consider graviton emission in the bulk for simply rotating black holes as well for black holes with all equal angular momenta.

Acknowledgments

H. K. was supported in part by Grants-in-Aid for Scientific Research from JSPS (No. 18540265). At the be-

ginning of this work R. A. K. was supported by the *Japan Society for the Promotion of Science (Japan)* and at the final stage by the *Alexander von Humboldt Foundation (Germany)* R. A. K. also acknowledges the hospitality of the Theory Division of the High Energy Accelerator Research Organization (KEK) in Tsukuba, where a part of this work was done. A. Z. was supported by *Fundação de Amparo à Pesquisa do Estado de São Paulo (FAPESP)*, Brazil.

-
- [1] R. Emparan and H. S. Reall, *Living Rev. Rel.* **11**, 6 (2008).
 [2] P. Kanti, arXiv:0802.2218 [hep-th].

- [3] H. Kodama, *Lect. Notes Phys.* **769**, 427 (2009) [arXiv:0712.2703 [hep-th]].
 [4] Kodama, H.: *Prog. Theor. Phys. Suppl.* **172**, 11–20

- (2008).
- [5] Kodama, H., Ishibashi, A. and Seto, O.: *Phys. Rev. D* **62**, 064022 (2000).
 - [6] H. Kodama and A. Ishibashi, *Prog. Theor. Phys.* **111**, 29 (2004).
 - [7] A. Ishibashi and H. Kodama, *Prog. Theor. Phys.* **110**, 901 (2003).
 - [8] H. Kodama and A. Ishibashi, *Prog. Theor. Phys.* **110** (2003) 701.
 - [9] R. A. Konoplya and A. Zhidenko, *Nucl. Phys. B* **777**, 182 (2007) [arXiv:hep-th/0703231].
 - [10] R. A. Konoplya and A. Zhidenko, *Phys. Rev. D* **78**, 104017 (2008) [arXiv:0809.2048 [hep-th]].
 - [11] R. A. Konoplya and A. Zhidenko, arXiv:0809.2822 [hep-th].
 - [12] T. Takahashi and J. Soda, arXiv:0902.2921 [gr-qc].
 - [13] M. Beroiz, G. Dotti and R. J. Gleiser, *Phys. Rev. D* **76**, 024012 (2007) [arXiv:hep-th/0703074]; R. J. Gleiser and G. Dotti, *Phys. Rev. D* **72**, 124002 (2005) [arXiv:gr-qc/0510069].
 - [14] R. A. Konoplya and A. Zhidenko, *Phys. Rev. D* **77**, 104004 (2008) [arXiv:0802.0267 [hep-th]].
 - [15] M. Kimura, K. Murata, H. Ishihara and J. Soda, *Phys. Rev. D* **77**, 064015 (2008) [arXiv:0712.4202 [hep-th]]; H. Ishihara, M. Kimura, R. A. Konoplya, K. Murata, J. Soda and A. Zhidenko, *Phys. Rev. D* **77**, 084019 (2008) [arXiv:0802.0655 [hep-th]].
 - [16] R. A. Konoplya, K. Murata, J. Soda and A. Zhidenko, *Phys. Rev. D* **78**, 084012 (2008) [arXiv:0807.1897 [hep-th]].
 - [17] S. R. Dolan, *Phys. Rev. D* **76**, 084001 (2007) [arXiv:0705.2880 [gr-qc]].
 - [18] H. K. Kunduri, J. Lucietti and H. S. Reall, *Phys. Rev. D* **74**, 084021 (2006) [arXiv:hep-th/0606076].
 - [19] K. Murata and J. Soda, arXiv:0803.1371 [hep-th].
 - [20] K. Murata, arXiv:0812.0718 [hep-th].
 - [21] H. Kodama, R. A. Konoplya and A. Zhidenko, arXiv:0812.0445 [hep-th].
 - [22] H. Suzuki, E. Takasugi and H. Umetsu, *Prog. Theor. Phys.* **100** (1998) 491 [arXiv:gr-qc/9805064]; R. A. Konoplya and A. Zhidenko, *Phys. Rev. D* **76**, 084018 (2007) [arXiv:0707.1890 [hep-th]].
 - [23] E. W. Leaver, *Proc. Roy. Soc. Lond.* **A402**, 285 (1985).
 - [24] A. Zhidenko, *Phys. Rev. D* **74**, 064017 (2006), [gr-qc/0607133]; R. A. Konoplya and A. Zhidenko, *Phys. Rev. D* **73**, 124040 (2006) [arXiv:gr-qc/0605013].
 - [25] B. F. Schutz and C. M. Will *Astrophys. J. Lett* **291** L33 (1985); S. Iyer and C. M. Will *Phys. Rev. D* **35** 3621 (1987).
 - [26] R. A. Konoplya, *Phys. Rev. D* **68**, 024018 (2003); R. A. Konoplya, *J. Phys. Stud.* **8**, 93 (2004).
 - [27] R. A. Konoplya, *Phys. Rev. D* **68**, 124017 (2003) [arXiv:hep-th/0309030].
 - [28] H. T. Cho, A. S. Cornell, J. Doukas and W. Naylor, arXiv:0904.1867 [gr-qc].
 - [29] E. Abdalla, O. P. F. Piedra and J. de Oliveira, arXiv:0810.5489 [hep-th]; M. l. Liu, H. y. Liu and Y. x. Gui, *Class. Quant. Grav.* **25**, 105001 (2008) [arXiv:0806.2716 [gr-qc]]; P. Kanti and R. A. Konoplya, *Phys. Rev. D* **73**, 044002 (2006) [arXiv:hep-th/0512257]; J. F. Chang, J. Huang and Y. G. Shen, *Int. J. Theor. Phys.* **46**, 2617 (2007); H. T. Cho, A. S. Cornell, J. Doukas and W. Naylor, *Phys. Rev. D* **77**, 016004 (2008) [arXiv:0709.1661 [hep-th]]; J. F. Chang and Y. G. Shen, *Int. J. Theor. Phys.* **46**, 1570 (2007); Y. Zhang and Y. X. Gui, *Class. Quant. Grav.* **23**, 6141 (2006) [arXiv:gr-qc/0612009]; R. A. Konoplya, *Phys. Lett. B* **550**, 117 (2002) [arXiv:gr-qc/0210105]; S. Fernando and K. Arnold, *Gen. Rel. Grav.* **36**, 1805 (2004) [arXiv:hep-th/0312041].
 - [30] P. Kanti, H. Kodama, R. A. Konoplya, N. Pappas and A. Zhidenko, arXiv:0906.3845 [hep-th].